Available online at www.sciencedirect.com
ScienceDirect
Journal of Computational Physics 222 (2007) 832–848
JOURNAL OF COMPUTATIONAL PHYSICS
www.elsevier.com/locate/jcp

Semi discrete discontinuous Galerkin methods and stage-exceeding-order, strong-stability-preserving Runge–Kutta time discretizations

Ethan J. Kubatko [a,*], Joannes J. Westerink [a], Clint Dawson [b]

[a] Department of Civil Engineering and Geological Sciences, University of Notre Dame, Notre Dame, IN 46556, United States
[b] Institute for Computational Engineering and Sciences, The University of Texas at Austin, Austin, TX 78712, United States

Received 26 April 2006; received in revised form 11 July 2006; accepted 21 August 2006
Available online 4 October 2006

Abstract

This paper investigates the use of a special class of strong-stability-preserving (SSP) Runge–Kutta time discretization methods in conjunction with discontinuous Galerkin (DG) finite element spatial discretizatons. The class of SSP methods investigated here is defined by the property that the number of stages s is greater than the order k of the method. From analysis, CFL conditions for the linear (L^2) stability of the methods defined using the $s > k$ SSP schemes are obtained that are less restrictive than those of the "standard" so-called RKDG methods that use $s = k$ SSP Runge–Kutta schemes. The improvement in the CFL conditions for linear stability of the methods more than offsets the additional work introduced by the increased number of stages. Given that the CFL conditions for linear stability are what must be respected in practice in order to maintain high-order accuracy, the use of the $s > k$ SSP schemes results in RKDG methods that are more efficient than those previously defined. Furthermore, with the application of a slope limiter, the nonlinear stability properties of the forward Euler method and the DG spatial discretization, which have been previously proven, are preserved with these methods under less restrictive CFL conditions than those required for linear stability. Thus, more efficient RKDG methods that possess the same favorable accuracy and stability properties of the "standard" RKDG methods are obtained. Numerical results verify the CFL conditions for stability obtained from analysis and demonstrate the efficiency advantages of these new RKDG methods.

Keywords: Discontinuous Galerkin; Strong-stability-preserving; Runge–Kutta

1. Introduction

The method of lines is a widely used approach for the solution of time dependent partial differential equations (PDEs). Upon application of a spatial discretization, the PDE is reduced to a system of ordinary

* Corresponding author. Tel.: +1 574 631 3864; fax: +1 574 631 9236.
E-mail address: ekubatko@nd.edu (E.J. Kubatko).

0021-9991/$ - see front matter
doi:10.1016/j.jcp.2006.08.005

differential equations (ODEs) in time – the semi discrete equations – that can then be solved using various time discretization methods. For a consistent, linear method, if the time discretization applied to the semi discrete equations is linearly stable then the method is convergent for problems with smooth solutions.

In the case of hyperbolic PDEs, where solutions may not be smooth, higher-order methods that are linearly stable may develop nonphysical oscillations in the presence of steep fronts or discontinuities. One common way of controlling these oscillations is through slope limiting, the application of which, renders the method nonlinear, even for linear problems. To prove convergence of nonlinear methods, some form of nonlinear stability property, such as requiring that the total variation of the numerical solution does not increase in time (the TVD property) or remains bounded in time (the TVB property), is also generally sought.

The design of high-order methods that are nonlinearly stable is possible through the use of a special class of high-order time discretization methods – what have come to be called strong-stability-preserving (SSP) methods (see, for example, the review articles [10,11,13]). Originally referred to as TVD time discretization methods, these time stepping schemes were first introduced by Shu and Osher [24] as a means of obtaining second-order accurate and higher time discretization methods that *preserve* the TVD property of a given spatial discretization and the first-order forward Euler method in time. Thus, to prove the TVD property of a method using these higher-order time discretizations, it is sufficient to show that the spatial discretization and the forward Euler method are TVD, which can be relatively easy to demonstrate. In fact, this class of higher-order time discretization methods will not only preserve the TVD property but will preserve the stability of the forward Euler method in any semi-norm or norm, hence the name SSP methods.

One particularly popular class of semi discrete finite element methods for the solution of hyperbolic conservation laws that use SSP time discretizations methods is the class of so-called Runge–Kutta discontinuous Galerkin (RKDG) methods first introduced by Cockburn and Shu [6]. As the name implies, the methods use DG finite element spatial discretizations and a special class of explicit SSP Runge–Kutta methods in time. In one-dimension, the methods can be rendered either TVDM (TVD in the means) or TVBM (TVB in the means) with the application of an appropriate slope limiter. In multiple dimensions, where the TVD property is incompatible with high-order accuracy [8], a maximum principle or L^∞ bound on the solution can be derived [5,28]. Along with these favorable numerical properties, the ease with which these methods can be coded and extended to higher-order accuracy has led to their wide spread use for a variety of problems including gas dynamics, contaminant transport, shallow water flow, and many other applications (see for example [1,15,17–19,23,27,29]).

Given that it is impossible to have implicit, unconditionally SSP Runge–Kutta methods of order greater than one [10,14], explicit SSP Runge–Kutta methods are typically used for higher-order time discretizations. It is well known that the time step used in such methods must satisfy a CFL condition for stability. In [6], assuming smooth solutions, a somewhat restrictive CFL condition for the linear stability of a second-order RKDG method (without the use of a slope limiter) for a linear, scalar conservation law in one-dimension was derived. This second-order RKDG method, which uses piecewise linear approximations in space and a two-stage, second-order SSP Runge–Kutta scheme, was also shown to be TVBM under a somewhat weaker CFL condition with the application of a slope limiter that renders the forward Euler step TVBM. This approach was generalized to kth order accurate RKDG methods in [4], which use kth stage, kth order accurate SSP Runge–Kutta time discretizations and a kth order accurate DG method. The CFL condition for TV stability in the general case was obtained along with the CFL condition for linear stability in the third-order case. As pointed out in [6] (and subsequently in [7]), although convergence of the RKDG methods is ensured under the CFL conditions for TV stability, it is the CFL conditions for linear stability of the methods, which are more restrictive than those required for TV stability, that must be respected in order to maintain higher-order accuracy. Thus, although it is the nonlinear stability that is highly sought after for theoretical reasons, it is ultimately the conditions for linear stability that must be respected in practice. Unfortunately, in the case of the RKDG methods, these conditions can be quite restrictive, especially for higher-order methods (see for example [7]).

In this paper, we investigate the use of a special class of SSP Runge–Kutta schemes in the framework of the RKDG method for which the number of stages s is greater than the order k of the time discretization. The use of these schemes is investigated with the goal of obtaining RKDG methods that have improved linear stability CFL constraints and, as such, are more efficient than the "standard" RKDG methods that use $s = k$ SSP

Runge–Kutta schemes. Given that the methods are SSP the nonlinear stability properties of the RKDG methods are guaranteed with the application of a slope limiter. The class of $s > k$ SSP Runge–Kutta methods was originally introduced by Spiteri and Ruuth [25] and further developed and analyzed in a series of papers [20,21,26]. In the case that a given spatial discretization and the forward Euler method are stable, these schemes are more efficient than the $s = k$ schemes due to the fact that the additional work that is required for the increased number of stages is offset by an improved CFL condition. In the case of the RKDG methods, although the forward Euler method is nonlinearly stable with the application of a slope limiter, the linear stability of the methods does not follow from the forward Euler step, and the stability of the complete Runge–Kutta step must be analyzed for each SSP scheme. We elaborate on this point in Section 4.

This paper is organized as follows. First, in Section 2, we consider the DG spatial discretization of the linear conservation law, or linear transport equation, in one space dimension. In Section 3, we present the general SSP Runge–Kutta time discretization method that is used in the RKDG method, and provide an overview of some of the important aspects of SSP Runge–Kutta methods. Then, in Section 4, we obtain CFL conditions for the linear stability of the RKDG methods using the $s > k$ SSP Runge–Kutta schemes presented in Section 3. From these results, the efficiency of these schemes are then determined relative to the standard $s = k$ schemes and optimal, in terms of computational efficiency, RKDG methods are identified. Finally, numerical results for both linear and nonlinear problems are presented in Section 5 that validate the stability analysis and demonstrate the efficiency advantages of these new RKDG methods.

2. The DG spatial discretization

In this section, we describe the DG spatial discretization of a linear, scalar conservation law, or linear transport equation, in one-dimension:

$$\frac{\partial u}{\partial t} + c\frac{\partial u}{\partial x} = 0, \quad (x,t) \in \Omega \times (0,T] \tag{1}$$

where c is a real positive constant, Ω is a domain in $\mathbb{R}^1$, and $T > 0$. Eq. (1) is supplemented with an initial-condition and suitable boundary conditions.

Given a partition of the domain Ω into elements $\Omega_j = (x_{j-1/2}, x_{j+1/2})$, a weak formulation of the problem is obtained by multiplying Eq. (1) by a test function v and integrating over Ω_j:

$$\int_{\Omega_j} \frac{\partial u}{\partial t} v \, \mathrm{d}x - \int_{\Omega_j} cu \frac{\mathrm{d}v}{\mathrm{d}x} \, \mathrm{d}x + cuv \Big|_{x_{j-1/2}}^{x_{j+1/2}} = 0 \tag{2}$$

where it is noted that the flux term has been integrated by parts.

The DG method is applied by approximating the true solution u by u_h and choosing a test function v that belongs to a finite-dimensional subspace U_h, which we take to be P^k, the space of polynomials of degree k defined over Ω_j. Due to the fact that C^0 continuity is not enforced between elements in the DG method, the flux $f = cu$ at the boundaries of Ω_j must be approximated by a *numerical flux* $\widehat{f}$, which in the present case can be defined by simple upwinding, that is

$$\hat{f}_{j\pm1/2} \equiv c\hat{u}_{j\pm1/2} \tag{3}$$

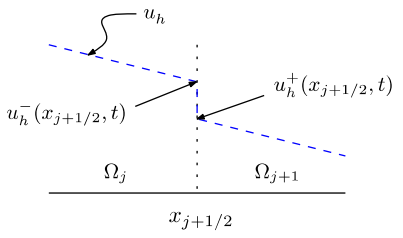

Fig. 1. Discontinuity of u_h at element interface.

where $\hat{u}_{j\pm1/2} = u_h^-(x_{j\pm1/2}, t)$ is the upwind value of the approximate solution at an element boundary – see Fig. 1.

A discrete weak form of the problem is then obtained by replacing the true solution u and the test function v by u_h, $v_h \in U_h$ and making use of the numerical flux defined by Eq. (3):

$$\int_{\Omega_j} \frac{\partial u_h}{\partial t} v_h \, \mathrm{d}x - \int_{\Omega_j} c u_h \frac{\mathrm{d}v_h}{\mathrm{d}x} \, \mathrm{d}x + c\hat{u}v_h \Big|_{x_{j-1/2}}^{x_{j+1/2}} = 0 \tag{4}$$

To proceed, a basis is chosen for the finite element space U_h. The Legendre polynomials $\{\phi_m\}$ are a particularly convenient choice and the solution $u_h \in P^k$ over an element takes the form

$$u_h|_{\Omega_j} = \sum_{m=0}^{k} (u_m)_j \phi_m \tag{5}$$

where $(u_m)_j$ are the degrees freedom of u_h in Ω_j.

The Legendre polynomials satisfy the following orthogonality relationship:

$$\int_{-1}^{1} \phi_m \phi_n \, \mathrm{d}\xi = \begin{cases} 0 & m \neq n \\ \frac{2}{2m+1} & m = n \end{cases} \tag{6}$$

The following identities are also useful:

$$\phi_m(\xi = -1) = (-1)^m, \quad \phi_m(\xi = 1) = 1 \tag{7}$$

Using (6) and (7) the discrete equations for an element Ω_j can be expressed in the following simple form:

$$\text{for } m = 0, 1, \ldots, k \quad \frac{\mathrm{d}}{\mathrm{d}t}(u_m)_j \equiv L_m = c \frac{2m+1}{\Delta x_j} \left\{ \int_{-1}^{1} u_h \frac{\mathrm{d}\phi_m}{\mathrm{d}\xi} \, \mathrm{d}\xi + (-1)^m \sum_{n=0}^{k} (u_n)_{j-1} - \sum_{n=0}^{k} (u_n)_j \right\} \tag{8}$$

where $\Delta x_j = x_{j+1/2} - x_{j-1/2}$.

Defining the following vectors:

$$\mathbf{u}_j \equiv [u_0, u_1, \ldots, u_k]^{\mathrm{T}} \tag{9}$$

$$\mathbf{L} \equiv [L_0, L_1, \ldots, L_k]^{\mathrm{T}} \tag{10}$$

the semi discrete equations can be written in the compact form

$$\sum_j \frac{\mathrm{d}}{\mathrm{d}t}(\mathbf{u}_j) = \mathbf{L}(\mathbf{u}_{j-1}, \mathbf{u}_j) \tag{11}$$

3. SSP Runge–Kutta schemes

In this section, we introduce the general form of the explicit s-stage SSP Runge–Kutta method that will be used to discretize the systems of ODEs obtained from the DG spatial discretization. We also give a brief review of some of the important aspects of SSP time discretization methods and define the relative efficiency of one scheme compared to another.

A general s-stage Runge–Kutta method applied to the systems of ODEs for an element given by Eq. (11) can be written in the form

$$\begin{aligned} \mathbf{u}_j^{(0)} &= \mathbf{u}_j^n \\ \mathbf{u}_j^{(i)} &= \sum_{l=0}^{i-1} \{\alpha_{il} \mathbf{u}_j^{(l)} + \Delta t \beta_{il} \mathbf{L}(\mathbf{u}_{j-1}^{(l)}, \mathbf{u}_j^{(l)})\}, \quad i = 1, 2, \ldots, s \\ \mathbf{u}_j^{n+1} &= \mathbf{u}_j^{(s)} \end{aligned} \tag{12}$$

where $\alpha_{il} \geqslant 0$ with $\alpha_{il} = 0$ only if $\beta_{il} = 0$. For consistency, we must have $\sum_{l=0}^{i-1} \alpha_{il} = 1,\ i = 1, 2, \ldots, s$. Additionally, α_{il} and β_{il} are subject to certain nonlinear constraints that correspond to the order of the Runge–Kutta method [25]. Note that if all the β_{il} are nonnegative then the method is simply a convex combination of forward Euler steps with time step sizes $\frac{\beta_{il}}{\alpha_{il}}\Delta t$. Following [25], we will refer to an s-stage, kth order accurate SSP Runge–Kutta scheme of the form (12) as an SSP(s,k) scheme. A kth order accurate RKDG method that uses an SSP(s,k) scheme and a kth order accurate DG spatial discretization (i.e. a $k-1$ degree polynomial) will be denoted as an SSP(s,k) RKDG method.

The defining feature of the SSP schemes is contained in the following important theorem [11]:

Theorem 3.1. *If the forward Euler method combined with the spatial discretization L is (strongly) stable under the CFL condition $\Delta t \leqslant \Delta t_{FE}$ then the Runge–Kutta method (12) with $\beta \geqslant 0$ preserves that stability under the CFL condition*:

$$\Delta t \leqslant \kappa \Delta t_{\mathrm{FE}} \tag{13}$$

where $\kappa \equiv \min(\frac{\alpha_{il}}{\beta_{il}})$.

The simple proof of this can be found, for example, in [7]. We note that the notion of strong stability, an example of which is the TVD property, implies that there is no temporal growth of the solution. This is in contrast to the general notion of stability, which allows bounded temporal growth. Both strong stability and general stability measures will be preserved by the high-order SSP methods [10].

Much of the research in the area of SSP methods has focused on finding optimal SSP Runge–Kutta schemes – that is, the Runge–Kutta scheme (12) for which κ is a maximum under the given constraints placed on the α_{il} and β_{il}. Optimal $s = k$ SSP Runge–Kutta methods with nonnegative β_{il} have been known for some time for $k = 2$ and 3 [24]. These schemes are in fact those that have been used previously in the literature to define second- and third-order RKDG methods, e.g. [4,5]. In [25], a new class of optimal SSP Runge–Kutta schemes with nonnegative β_{il} were introduced where the number of stages exceeds the order of the scheme, i.e. $s > k$. These schemes were further developed and analyzed in [20,21,26]. Assuming stability of the forward Euler method in conjunction with a given spatial discretization L, these schemes were found to be ultimately more efficient than the previously known optimal $s = k$ schemes due to the fact that the improvement in the CFL condition more than offset the additional work introduced by the increased number of stages. We provide a brief summary of this work.

In [25], optimal first- and second-order SSP Runge–Kutta schemes with an arbitrary number of stages s were given as well as an optimal SSP(4,3) scheme. Numerically optimized SSP(5, 3) and SSP(5,4) schemes were also given. The optimality of the SSP(5, 3) and SSP(5,4) schemes were later guaranteed in [20], which also gave several new numerically optimized third-order schemes that were guaranteed to be optimal: SSP(6, 3), SSP(7, 3), and SSP(8, 3). Finally, in [26], SSP$(s,4)$ schemes for $s = 6$, 7, and 8 were developed. In Tables 1 and 2, we list the α_{il} and β_{il} for the first few optimal SSP Runge–Kutta schemes of order 2 and 3, respectively. With the exception of the $s = k = 2$, 3 schemes, none of these schemes have been analyzed or used in the context of the RKDG methods.

As already pointed out, all of the above mentioned SSP Runge–Kutta schemes have only nonnegative β_{il}. The introduction of a negative β_{il} necessitates the introduction of a related spatial operator $\widetilde{L}$. Numerically, the only difference in computing L and $\widetilde{L}$ is a change in upwind direction (see for example [11]). Note that if L and $\widetilde{L}$ must be computed in the same stage then, in general, the computational cost as well as the storage

Table 1
The first two optimal second-order SSP Runge–Kutta schemes

Stages	α_{il}			β_{il}			$\min(\alpha_{il}/\beta_{il})$
2	1			1			1
	$\frac{1}{2}$	$\frac{1}{2}$		0	$\frac{1}{2}$		
3	1			$\frac{1}{2}$			2
	0	1		0	$\frac{1}{2}$		
	$\frac{1}{3}$	0	$\frac{2}{3}$	0	0	$\frac{1}{3}$	

Table 2
The first two optimal third-order SSP Runge–Kutta schemes

Stages	α_{il}				β_{il}				$\min(\alpha_{il}/\beta_{il})$
3	1				1				1
	$\frac{1}{3}$	$\frac{1}{4}$			0	$\frac{1}{4}$			
	$\frac{1}{3}$	0	$\frac{2}{3}$		0	0	$\frac{2}{3}$		
4	1				$\frac{1}{2}$				2
	0	1			0	$\frac{1}{2}$			
	$\frac{2}{3}$	0	$\frac{1}{3}$		0	0	$\frac{1}{6}$		
	0	0	0	1	0	0	0	$\frac{1}{2}$	

for that stage are doubled (in [12] it is pointed out that for some spatial discretizations it is possible to compute $\widetilde{L}$ at a lower cost). For this reason, negative β_{il} were generally avoided in the search for optimal SSP schemes. Indeed, it was later verified in [21] that many of the optimal nonnegative β_{il} SSP Runge–Kutta schemes are also optimal when negative β_{il} are considered in the search for optimal schemes as well. However, it is not always possible to avoid negative β_{il}. In fact, it was proven in [9] that any four stage, fourth-order SSP Runge–Kutta method must have at least one negative β_{il}. Furthermore, it was proven in [22] that any fifth-order or greater SSP Runge–Kutta scheme will also require negative β_{il}. In this paper, we restrict our attention to SSP Runge–Kutta schemes with nonnegative β_{il} with the exception of comparing the aforementioned fourth-order SSP Runge–Kutta schemes with $s > 4$ developed in [26], which have all nonnegative β_{il}, with the optimal SSP(4,4) scheme given in [12], which has two negative β_{il}.

To conclude this section, we define the relative efficiency, RE of one scheme to another. The efficiency of scheme m relative to scheme n is given by

$$\mathrm{RE} \equiv 1 - \left(\frac{s_m^*}{s_n^*}\right)\left(\frac{v_n^*}{v_m^*}\right) \tag{14}$$

where s_m^* and s_n^* are the number of effective stages of the two methods that are being compared and v_m^* and v_n^* are the maximum Courant numbers $v \equiv c\frac{\Delta t}{\Delta x}$ that can be used for stability for the two methods, i.e. $v \leqslant v^*$. For methods with nonnegative β_{il}, the number of effective stages s^* is simply equal to the number of stages s of the scheme, i.e. each stage requires one function evaluation of L. However, the optimal SSP(4,4) scheme requires 4 function evaluations of L, one for each stage, and one additional function evaluation of $\widetilde{L}$ or effectively 5 stages.

Note that there are two competing factors that determine the efficiency of one scheme relative to another. On the one hand, with an increase in the number of effective stages ($s_m^* > s_n^*$) the work load increases by a factor of s_m^*/s_n^*. On the other hand, the CFL condition improves with an increase in the number of stages so that for a given spatial grid only v_n^*/v_m^* as many time steps are required to reach a given time T if the maximum allowable time step of the method is used. Thus, as long as the product of these two factors is less than one, scheme m will be more efficient than scheme n.

4. Stability analysis

4.1. Linear stability

Presently, we wish to examine the conditions necessary for the linear stability of the RKDG methods using the $s > k$ SSP Runge–Kutta schemes introduced in the previous section with the goal of obtaining more efficient RKDG methods. To this end, we consider the first stage of an SSP Runge–Kutta scheme applied to Eq. (11):

$$\begin{aligned} \mathbf{u}_j^{(0)} &= \mathbf{u}_j^n \\ \mathbf{u}_j^{(1)} &= \alpha_{10}\mathbf{u}_j^{(0)} + \Delta t\beta_{10}\mathbf{L}(\mathbf{u}_{j-1}^{(0)}, \mathbf{u}_j^{(0)}) \end{aligned} \tag{15}$$

Using Eq. (8) this can written in the form

$$\mathbf{u}_j^{(1)} = \mathbf{A}\mathbf{u}_{j-1}^{(0)} + \mathbf{B}\mathbf{u}_j^{(0)} \tag{16}$$

where $\mathbf{A}$ and $\mathbf{B}$ are matrices of size $(k+1)\times(k+1)$ for a P^k DG method. For example, for a P^1 DG spatial discretization $\mathbf{A}$ and $\mathbf{B}$ are

$$\mathbf{A} = \beta_{10} v \begin{bmatrix} 1 & 1 \\ -3 & -3 \end{bmatrix}, \quad \mathbf{B} = \alpha_{10}\mathbf{I} - \beta_{10} v \begin{bmatrix} 1 & 1 \\ -3 & 3 \end{bmatrix} \tag{17}$$

and for P^2:

$$\mathbf{A} = \beta_{10} v \begin{bmatrix} 1 & 1 & 1 \\ -3 & -3 & -3 \\ 5 & 5 & 5 \end{bmatrix}, \quad \mathbf{B} = \alpha_{10}\mathbf{I} - \beta_{10} v \begin{bmatrix} 1 & 1 & 1 \\ -3 & 3 & 3 \\ 5 & -5 & 5 \end{bmatrix} \tag{18}$$

where $\mathbf{I}$ is the identity matrix.

We consider the domain $\Omega = [0,1]$ with periodic boundary conditions. Applying the ideas of classic Von Neumann stability analysis, we consider a single Fourier component of the solution:

$$\mathbf{u}_j^n = \widetilde{\mathbf{u}}_j(t) \mathrm{e}^{\mathrm{i}\theta_j} \tag{19}$$

where $\widetilde{\mathbf{u}}_j$ is a vector of length $(k+1)$, $\mathrm{i} = \sqrt{-1}$, and $\theta_j = \zeta j \Delta x_j$, where ζ is the wave number and $j = 1, 2, \ldots, N$ where N is the number of elements. We are considering a uniform finite element grid, i.e. each $\Delta\, x_j = 1/N$. Applying the first stage of an SSP Runge–Kutta scheme to Eq. (19) gives:

$$\mathbf{u}_j^{(1)} = [\mathbf{A}\mathrm{e}^{-\mathrm{i}\theta_j} + \mathbf{B}]\mathbf{u}_j^{(0)} = \mathbf{G}\mathbf{u}_j^{(0)} \tag{20}$$

where $\mathbf{G} \equiv \mathbf{A}\mathrm{e}^{-\mathrm{i}\theta_j} + \mathbf{B}$ is the amplification matrix of the first stage. Using this notation, an s-stage, second-order Runge–Kutta method can be written in the form

$$\mathbf{u}_j^{n+1} = \underbrace{\left[\frac{1}{s}\mathbf{I} + \frac{s-1}{s}\mathbf{G}^s\right]}_{\mathbf{G}^*} \mathbf{u}_j^n \tag{21}$$

where $\mathbf{G}^s$ is used to denote $\mathbf{G}$ to the power of s and $\mathbf{G}^*$ is the amplification matrix of the complete Runge–Kutta method. Similar expressions can also be obtained for the various third- and fourth-order Runge–Kutta methods examined here. For example, the complete SSP(3,3) scheme can be written as

$$\mathbf{u}_j^{n+1} = \underbrace{\left[\frac{1}{3}\mathbf{I} + \frac{1}{2}\mathbf{G} + \frac{1}{6}\mathbf{G}^3\right]}_{\mathbf{G}^*} \mathbf{u}_j^n \tag{22}$$

To prove linear stability of the RKDG methods it must either be shown that the forward Euler method is stable in conjunction with a given DG spatial discretization, which, from Theorem 3.1, it would follow that all of the SSP Runge–Kutta schemes give stable RKDG methods or, short of this, that the complete Runge–Kutta scheme is stable. That is, it must be shown that the following condition holds for some $v > 0$:

$$\max(|\lambda_{G^*}|) \leqslant 1 \tag{23}$$

where $|\lambda_{G^*}|$ represents the modulus of the eigenvalues λ_{G^*} of the amplification matrix $\mathbf{G}^*$ of the complete Runge–Kutta method. We note that the eigenvalues λ_{G^*} are merely functions of the eigenvalues λ_G of the amplification matrix G as defined in Eq. (20). For example, the λ_{G^*} for a given s-stage, second-order SSP Runge–Kutta scheme are given by the function:

$$F_{s,2}(\lambda_G) \equiv \lambda_{G^*} = \frac{1}{s} + \frac{s-1}{s}\lambda_G^s \tag{24}$$

which is a direct consequence of Eq. (21).

The linear stability of the SSP(2,2) RKDG method was examined by Cockburn and Shu [6] where it was proven that the method is linearly stable under the rather restrictive CFL condition $v \leqslant 1/3$. The results of that

analysis are most clearly conveyed via Fig. 2, which shows a plot of the eigenvalues of the matrix $\mathbf{G}$ and those of $\mathbf{G}^*$ for $v = 1/3$ in the complex plane. From this figure, it can be seen that the forward Euler method, the first stage of the SSP(2, 2) scheme, is unstable for $v = 1/3$, i.e. part of the curve of the eigenvalues of $\mathbf{G}$ lies outside of the unit circle. In fact, it has been proven (see [3]) that this will be true for any $v > 0$ from which it follows that the forward Euler method is *unconditionally-unstable* in conjunction with a P^1 DG spatial discretization for a fixed v. This result carries over to all P^k DG spatial discretizations for $k \geqslant 1$ [7].

This result has an important consequence. Due to the fact that the forward Euler method is unstable, the linear stability of the RKDG method does not follow from Theorem 3.1, and the complete Runge–Kutta scheme must be analyzed for each case. Returning to the case of the stability of the SSP(2, 2) RKDG method, it can be seen in Fig. 2 that the second stage of the Runge–Kutta scheme has a stabilizing effect in the sense that the function $F_{2,2}$ given by Eq. (24) with $s = 2$, acts to push the curve of the eigenvalues λ_G into the unit circle, which results in a stable scheme.

The general SSP(s, 2) RKDG method can be examined in the same manner. For example, Fig. 3 shows a plot of the eigenvalues of $\mathbf{G}$ (the first-stage), $\mathbf{G}^2$ (the second stage), and $\mathbf{G}^*$ (the final stage) of the SSP(3, 2) Runge–Kutta scheme again for $v = 1/3$. Note that in this case the second stage acts to expand the curve of the eigenvalues of $\mathbf{G}$ so that they enclose a larger portion of the unit circle and then the final stage pushes this curve into the unit circle again resulting in a stable scheme. The other $s > 2$, second-order SSP Runge–Kutta schemes show similar behavior in which the second to $(s-1)$th stages act to expand the curves of the eigenvalues of the previous stage to enclose increasingly larger portions of the unit circle while the final stage pushes the curve of the eigenvalues of the $(s-1)$th stage into the unit circle.

It should be pointed out that it has not been attempted here to rigorously prove the stability of these schemes. Rather, the stability has been examined by first obtaining analytical expressions of the eigenvalues of G^* as functions of v and θ, and then checking the condition given by (23) at a discrete number of points for $\theta \in [0, 2\pi]$ for a fixed value of v. If condition (23) is satisfied for a given v for all values of θ then v is increased by a small increment until condition (23) is violated. The CFL condition is then given by the largest value of v for which condition (23) is satisfied. The results obtained with this procedure show excellent agreement with the CFL condition that can be used in practice, which is demonstrated in the next section, and agree well with results previously obtained for the SSP(2, 2) and SSP(3, 3) RKDG methods.

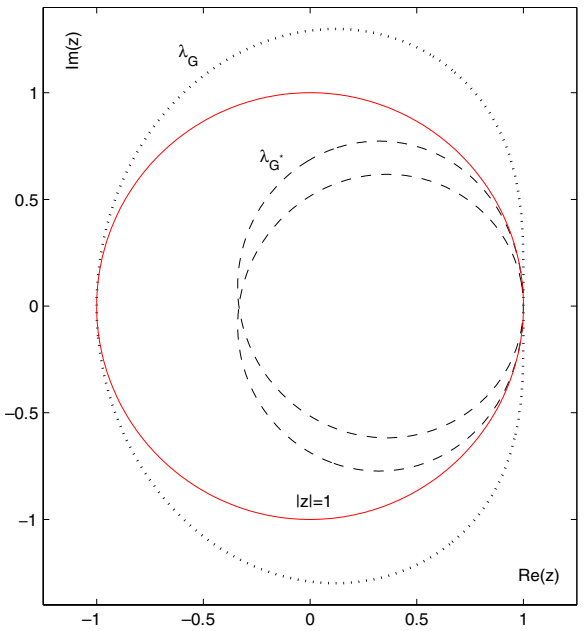

Fig. 2. The eigenvalues of $\mathbf{G}$ and $\mathbf{G}^*$ for $v = 1/3$ for the SSP(2, 2) RKDG method.

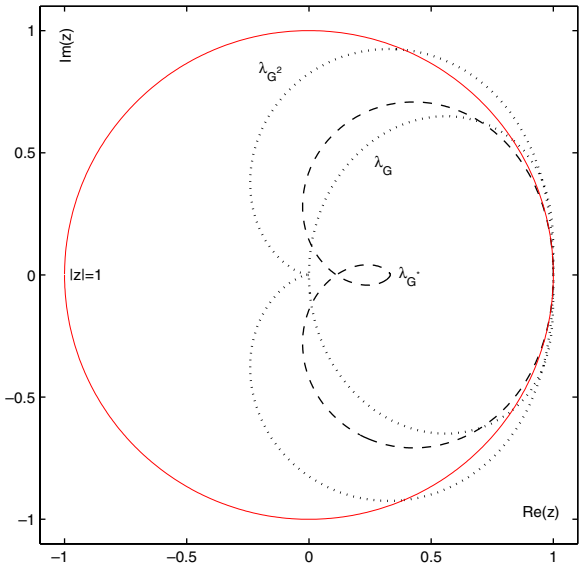

Fig. 3. The eigenvalues of $\mathbf{G}$, $\mathbf{G}^2$, and $\mathbf{G}^*$ for $v = 1/3$ for the SSP(3,2) RKDG method.

Using this approach, the CFL conditions necessary for the linear stability of the SSP(s,2) RKDG methods are obtained, which are summarized in Table 3. The computational savings that are offered by the $s > k = 2$ schemes relative to the $s = k = 2$ scheme are also reported. It can be seen that all of the schemes up to $s = 6$ are computationally more efficient than the standard second-order RKDG method and that the SSP(3,2) RKDG method provides the optimal second-order RKDG method with a 15% savings in efficiency over the SSP(2,2) RKDG method. In Figs. 4 and 5, the eigenvalues of $\mathbf{G}^*$ for the SSP(3,2) and SSP(4,2) schemes, respectively, for v equal to the CFL conditions reported in Table 3 are plotted in the complex plane. It can be seen that the eigenvalues of the amplification matrices $\mathbf{G}^*$ take up larger portions of the unit circle as the number of stages is increased.

The SSP(s,3) and SSP(s,4) RKDG methods are analyzed in the same way and are summarized in Table 3 as well. For the SSP(s,3) RKDG methods all of the schemes analyzed are more efficient than the popular SSP(3,3) scheme. In this case, the optimal RKDG method is obtained by using two additional stages, $s = 5$ and provides a nearly 18% increase in efficiency over the standard third-order RKDG method. The CFL condition for the SSP(3,3) RKDG method reported in Table 3 is the theoretical value found in [4] (a slightly larger value of 0.2092 was obtained using the method described here and, in fact, seems to be closer to the value that can be used in practice). For the SSP(s,4) RKDG methods we compare the efficiency of the $s > 4$ schemes relative to the optimal SSP(4,4) scheme given in [12], which has two negative β_{ik} and requires one function evaluation of $\widetilde{L}$. In this case, more significant savings in computational cost are obtained with the $s > k$

Table 3
CFL conditions and RE for the SSP(s,k) RKDG methods

Stages, s	SSP(s,2)		SSP(s,3)		SSP(s,4)	
	CFL	RE (%)	CFL	RE (%)	CFL	RE (%)
2	0.3333	...	...	...	...	...
3	0.5882	15.00[a]	0.2000	...	...	...
4	0.7611	12.42	0.3061	12.88	0.1696	...
5	0.8966	7.06	0.4060	17.90[a]	0.2152	21.19
6	1.0089	0.89	0.4842	17.39	0.2747	25.91
7	1.1052	−5.09	0.5667	17.65	0.3214	26.12
8	1.1895	−12.08	0.6444	17.24	0.3707	26.80[a]

[a] Optimal.

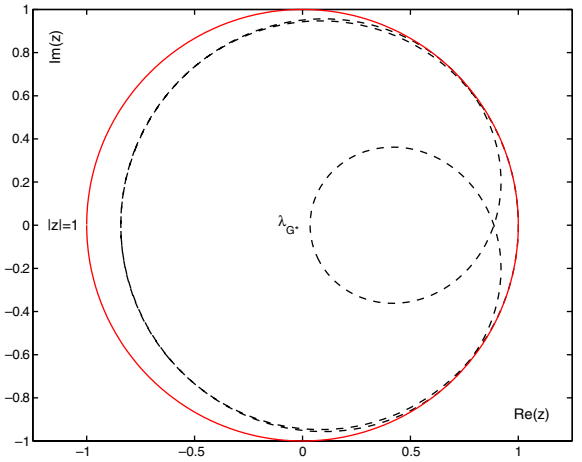

Fig. 4. The eigenvalues of $\mathbf{G}^*$ for $v = 0.5882$ for the SSP(3,2) RKDG method.

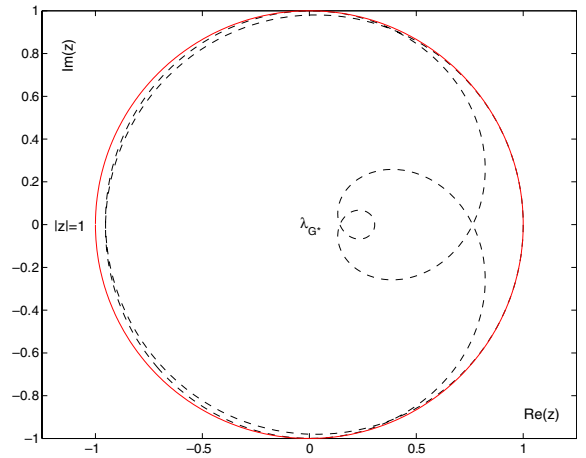

Fig. 5. The eigenvalues of $\mathbf{G}^*$ for $v = 0.7611$ for the SSP(4,2) RKDG method.

schemes with the optimal scheme, $s = 8$ providing a 27% savings in computational efficiency. We note the α_{il} and β_{il} for the SSP(3,2) scheme, which gives the optimal second-order RKDG method, are listed in Table 2 – see [20] for the SSP(5,3) and [26] for the SSP(8,4) α_{il} and β_{il}, which produce optimal third- and fourth-order RKDG methods, respectively.

We conclude this section by noting that the stability analysis has been presented in the somewhat nonstandard fashion used in [6] in order to draw analogies with that work. A more common way of presenting the results would be to plot the region of absolute stability of the Runge–Kutta method alongside the eigenvalues of the DG spatial discretization L times Δt. The region of absolute stability of the Runge–Kutta method is the set R_s in the complex plane for which $|P_s(z)| \leqslant 1$ where $P_s(z)$ is the characteristic polynomial of Runge–Kutta method (see for example [2]). Following this approach, the absolute stability regions for a number of the SSP$(s,2)$ and SSP$(s,3)$ schemes along with Δt times the eigenvalues of the corresponding DG spatial discretization are shown in Figs. 6 and 7, respectively, for given Courant numbers. With either method of presentation, of course, the end results of the analysis are the same.

4.2. Nonlinear stability

With the application of the generalized slope limiter described in [4], it can be proven that the forward Euler method in conjunction with a P^k DG spatial discretization with $k \geqslant 1$ is TVBM in one dimension under an

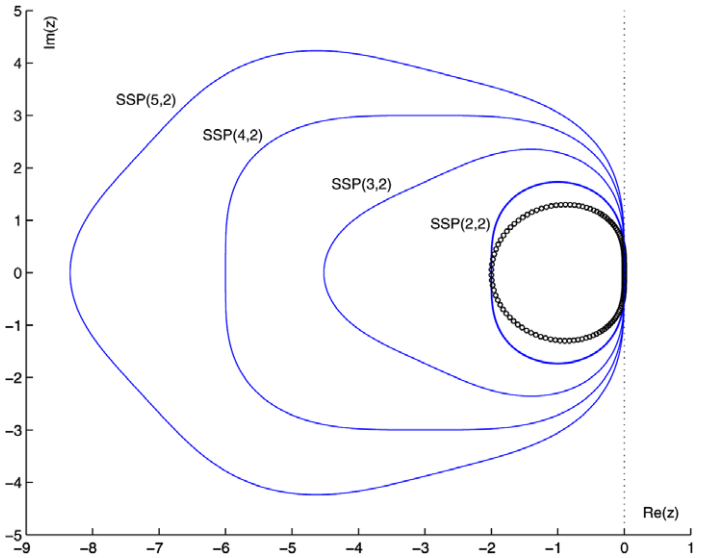

Fig. 6. Regions of stability for the SSP$(s,2)$ schemes (solid lines); The eigenvalues of L times Δt for $v = 0.3333$ (open circles).

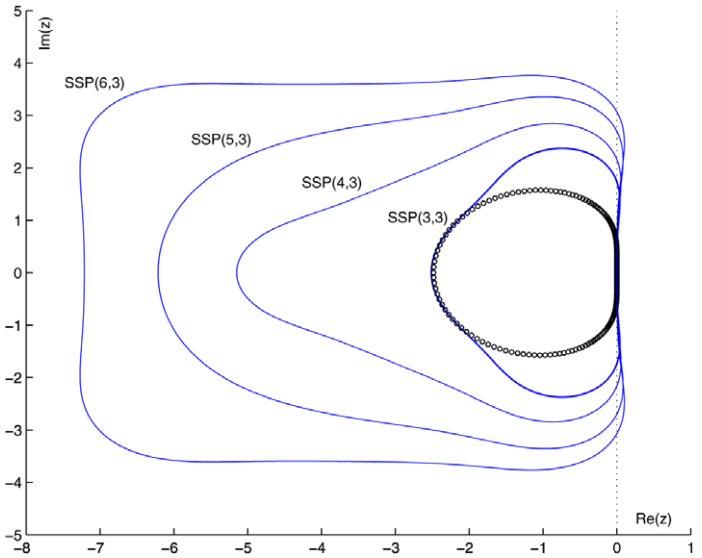

Fig. 7. Regions of stability for the SSP$(s,3)$ schemes (solid lines); The eigenvalues of L times Δt for $v = 0.2000$ (open circles).

appropriate CFL condition. For the linear conservation law this condition is $v \leqslant \kappa/2$ (see [7]) where κ is defined in Theorem 3.1. Given that the forward Euler method can be rendered TV-stable with the slope limiter, the TV-stability of RKDG methods using any of the higher-order SSP Runge–Kutta schemes follow from Theorem 3.1. In all cases examined here, the conditions required for TV-stability are much weaker than those required for linear stability. However, as pointed out in [7], it is the linear stability condition that must be respected or the high-order accuracy of the methods will degenerate to first-order. This will be demonstrated in the next section in the numerical examples. In two-dimensions, the DG spatial discretization in conjunction with the forward Euler method can be shown to satisfy a maximum principle with the application of an appropriate slope limiting procedure [5,28]. The SSP Runge–Kutta schemes examined here will maintain this maximum principle as well.

5. Numerical results

In this section, we apply the various SSP(s,k) RKDG methods to two test problems. Although the analysis in the previous section was limited to a linear, scalar equation, the test problems considered in this section consist of both linear and nonlinear scalar equations. We examine problems with both continuous and discontinuous solutions. We are interested in examining several aspects of the methods: testing the linear stability limits obtained for the $s > k$ schemes, comparing the efficiency gains that are predicted from the analysis with those that can be obtained in practice, verifying the order of convergence of the $s > k$ schemes, and evaluating the performance of the schemes in the presence of discontinuities.

5.1. Test Case 1: linear advection of a sine wave

The first test case examines the linear advection of a sine wave. We solve Eq. (1) with $c = 1$ on the domain $\Omega = [0,1]$ with periodic boundary conditions and the following initial condition:

$$u(x,0) = \sin\left(\frac{2\pi x}{L}\right) \tag{25}$$

where we take $L = 1$ for this problem. A uniform grid with $\Delta x = 0.02$ (50 elements) is used, and the problem is run to $T = 50$ so that the initial condition crosses the domain 50 times. This problem is well suited to examine the amplitude and phase properties of the various methods.

Tables 4–6 summarize the results of the numerical testing of the various schemes. We compare the maximum allowable time steps that can be used in practice with those predicted by the analysis, the efficiency rates that are realized in practice with those predicted, and the L^2, phase, and amplitude errors of the different schemes. For the SSP($s,2$) schemes we have only examined those that theoretically offer computational savings over the SSP(2,2) scheme, that is, the schemes up to and including $s = 6$ (see Table 3).

With respect to the CFL conditions and efficiencies, it can be observed that very good agreement is obtained between the values that are realized in practice (labeled CFL Num. and RE Num. in the table) with those obtained from the analysis (labeled CFL Theor. and RE Theor. in the table). The CFL conditions that could be used in practice were obtained by increasing ν by 0.0001, starting from the value obtained from the analysis, until the code went completely unstable, i.e. returned a value of NaN. The efficiencies obtained in practice were computed as a ratio of the CPU times measured from runs for each scheme using the maximum allowable time step permitted by the theoretical CFL conditions obtained in the previous section. The small discrepancy observed in the theoretical and numerical efficiencies, which increases as the number of stages increases, is most likely due to the adverse effects of additional stage storage on the computational efficiency of the code.

The errors were computed at the final time of the simulation. Each simulation used for computing the errors was also run using the maximum allowable time step based on the CFL conditions obtained from the analysis. The amplitude errors that are reported are a point measure comparing the maximum value of the exact solution ($u = 1$) with the maximum value of the numerical solution computed at a discrete number of points. The phase errors are also a point measure comparing the distance traveled by the point of the exact solution initially at $x = 0.50$ to the distance traveled by the point of the numerical solution closest to this point

Table 4
Comparison of the SSP($s,2$) RKDG methods

$k = 2$ s	CFL		RE (%)		Errors		
	Theor.	Num.	Theor.	Num.	L^2	Amp.	Phase
2	0.3333	0.3335	···	···	6.50E−02	3.28E−03	1.35E−02
3	0.5882	0.5882	15.00	14.48	1.01E−01	2.67E−03	2.27E−02
4	0.7611	0.7613	12.42	10.97	1.28E−01	1.53E−04	2.53E−02
5	0.8966	0.8968	7.06	4.85	1.17E−01	8.91E−04	2.69E−02
6	1.0089	1.0091	0.89	−2.29	1.19E−01	1.17E−03	2.76E−02

Table 5
Comparison of the SSP(s,3) RKDG methods

$k=3$ s	CFL		RE (%)		Errors		
	Theor.	Num.	Theor.	Num.	L^2	Amp.	Phase
3	0.2000	0.2097	...	...	1.48E−04	2.53E−04	2.61E−04
4	0.3061	0.3062	12.88	12.43	2.64E−04	3.74E−04	2.77E−04
5	0.4060	0.4061	17.90	16.80	3.02E−04	4.42E−04	−5.06E−04
6	0.4842	0.4842	17.39	15.76	3.28E−04	4.65E−04	1.59E−04
7	0.5667	0.5667	17.65	15.48	3.39E−04	5.02E−04	6.00E−05
8	0.6444	0.6444	17.24	14.33	3.58E−04	5.14E−04	−1.06E−03

Table 6
Comparison of the SSP(s,4) RKDG methods

$k=4$ s	CFL		RE (%)		Errors		
	Theor.	Num.	Theor.	Num.	L^2	Amp.	Phase
4	0.1696	0.1696	...	...	3.89E−07	3.74E−06	5.71E−04
5	0.2152	0.2152	21.19	18.97	4.80E−07	2.21E−05	1.71E−04
6	0.2747	0.2747	25.91	23.38	5.83E−07	1.32E−06	−1.06E−03
7	0.3214	0.3214	26.12	23.01	6.74E−07	3.42E−05	−1.90E−04
8	0.3707	0.3707	26.80	23.21	8.14E−07	7.13E−06	−1.11E−03

at the end of the simulation. A positive phase error corresponds to a phase lead while a negative number corresponds to a phase lag.

Referring to Tables 4–6, it can be seen that the errors are generally on the same order of magnitude for an RKDG method of a given order. We note, however, that in general there is an increase in the L^2 error levels as the number of stages of the scheme increases, which may be associated with either the increase in the Courant number or the error properties of the higher stage SSP Runge–Kutta schemes. For the second-order methods, inspection of the errors reveals that, at this level of grid resolution, the increases in error are mainly due to an increase in phase error. In fact, the amplitude errors actually decrease as a result of increasing the number of stages. In the case of the third- and fourth-order methods, both the amplitude and phase errors generally increase as result of increasing the number of stages, with the phase errors increasing by a larger factor than the amplitude errors. However, the error levels are generally very comparable.

Finally, as a demonstration of the degradation of high-order accuracy that can occur if the CFL condition for linear stability is violated while remaining below the CFL condition for TV-stability, which is much weaker than the condition for linear stability, we examine the convergence of the $s=k$ second- and third-order RKDG methods under these different time step restrictions, which are summarized in Table 7 (see also [7]). To ensure the TV-stability, the TVB minmod slope limiter of [4] is used (the parameter M of the slope limiter is set as suggested in that work). The errors and convergence rates are summarized in Tables 8 and 9, and although the calculations remain TV-stable for the larger time steps, it can clearly be seen that the high-order accuracy of the schemes is lost if the CFL conditions for linear stability are violated. Thus, even for this simple problem, one can see the importance of performing the linear stability analysis for these schemes, which were designed to preserve nonlinear stability, given that it is the CFL condition for linear stability that must be respected in order to maintain high-order accuracy. Lastly, although not shown here for this problem, all

Table 7
CFL conditions for the SSP(2,2) and SSP(3,3) RKDG methods

s,k	CFL_{L^2}	$\mathrm{CFL}_{\mathrm{TV}}$
2,2	1/3	1/2
3,3	1/5	1/2

Table 8
Order of convergence of the SSP(2,2) RKDG method for $v = 1/3$ and $v = 1/2$

Δx	SSP(2,2), $v = 1/3$		SSP(2,2) $v = 1/2$	
	Error	Order	Error	Order
1/50	6.50E−02	···	6.97E−01	···
1/100	1.62E−02	2.00	3.64E−01	0.94
1/200	4.06E−03	2.00	1.27E−01	1.52

Table 9
Order of convergence of the SSP(2,2) RKDG method for $v = 1/5$ and $v = 1/2$

Δx	SSP(3,3), $v = 1/5$		SSP(2,2) $v = 1/2$	
	Error	Order	Error	Order
1/50	1.48E−04	···	5.11E−01	···
1/100	1.84E−05	3.01	2.88E−01	0.83
1/200	2.30E−06	3.00	1.07E−01	1.43

of the schemes converged at the expected rates when the time steps satisfied the linear stability CFL conditions.

5.2. Test Case 2: evolution of a sine wave using Burgers' equation

In this test case, we apply the RKDG methods to a nonlinear problem by examining the evolution of a sine wave using Burgers' equation. We use the same initial condition as the previous problem this time with $L = 200$ and periodic boundary conditions. At time $t = \frac{100}{\pi}$ a discontinuity forms in the solution at $x = 100$. With this problem, we examine the order of convergence of both the standard $s = k$ and optimal RKDG methods established in the previous section. We are also interested in evaluating the performance of the methods in the presence of discontinuities.

First, the second-order RKDG methods are examined. The problem is run to $T = 32$ right after the formation of the shock on four uniform meshes with element lengths of $h = 2$, 1, 0.5, 0.25, i.e. using 100, 200, 400, and 800 elements, respectively. The order of convergence in the L^2 norm of both the SSP(2,2) and SSP(3,2) RKDG methods is computed at $t = 24$ while the solution is still smooth (see Fig. 8). Table 10 summarizes the

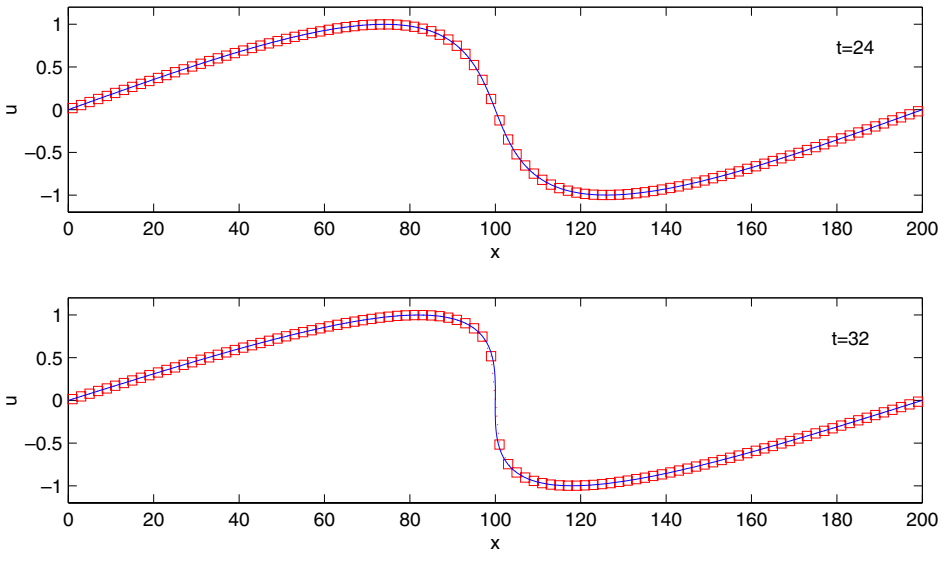

Fig. 8. Plots showing the exact solution (solid) and SSP(3,2) RKDG solution (squares) of test Case 2.

Table 10
Order of convergence of the SSP(2,2) and SSP(3,2) RKDG methods

Δx	SSP(2,2)		SSP(3,2)	
	Error	Order	Error	Order
2.00	9.68E−03	···	9.72E−03	···
1.00	2.58E−03	1.91	2.59E−03	1.91
0.50	6.71E−04	1.94	6.74E−04	1.94
0.25	1.71E−04	1.97	1.72E−04	1.97

results where it can be observed that second-order convergence is obtained with both methods with very similar errors. The SSP(2,2) scheme was run using $\frac{\Delta t}{\Delta x} = 0.3333$ while $\frac{\Delta t}{\Delta x} = 0.5882$ was used with the SSP(3,2) scheme. Fig. 8 demonstrates the performance of the SSP(3,2) RKDG method after the formation of the discontinuity. Again, the TVB limiter of Cockburn and Shu [4] is applied. Note that the discontinuity is resolved without the introduction of spurious oscillations demonstrating that the $s > k$ RKDG methods preserve the nonlinear stability properties of the forward Euler step, as they should.

The third- and fourth-order RKDG methods are examined in the same way. Again, in each case we examine the standard $s = k$ RKDG methods and the optimal RKDG methods defined in the previous section. For the third-order case, the optimal RKDG method is given by using the SSP(5,3) scheme. For the fourth-order case, theoretically, the optimal RKDG method is obtained using the SSP(8,4) scheme though only marginal increases in efficiency are gained compared to the SSP(6,4) and SSP(7,4) schemes. Indeed, it was shown in the previous test case that in practice the SSP(6,4) scheme actually appears to be the optimal scheme. Therefore, the SSP(4,4) scheme is compared to the SSP(6,4) scheme for this test case.

Tables 11 and 12 summarize the results of the convergence studies. The maximum allowable time steps were used in each case. The third-order schemes were run with $\frac{\Delta t}{\Delta x} = 0.2000$ and $\frac{\Delta t}{\Delta x} = 0.4060$ for the SSP(3,3) and SSP(5,3) schemes, respectively. The fourth-order schemes were run with $\frac{\Delta t}{\Delta x} = 0.1696$ and $\frac{\Delta t}{\Delta x} = 0.2747$ for the SSP(4,4) and SSP(6,4) schemes, respectively. Again, nearly optimal rates of convergence are obtained using both the $s = k$ and $s > k$ RKDG methods. We note that for this test case the errors of the optimal and standard RKDG methods are very similar. In particular, for the third-order case the error levels for the SSP(5,3) scheme are slightly lower than the SSP(3,3) scheme for this problem. Although not shown here, the optimal third- and fourth-order RKDG methods also accurately capture the discontinuity that forms in the solutions without oscillations.

Table 11
Order of convergence of the SSP(3,3) and SSP(5,3) RKDG methods

Δx	SSP(3,3)		SSP(5,3)	
	Error	Order	Error	Order
2.00	3.74E−04	···	3.18E−04	···
1.00	5.18E−05	2.85	5.09E−05	2.85
0.50	7.06E−06	2.88	6.94E−06	2.88
0.25	9.42E−07	2.91	9.25E−07	2.91

Table 12
Order of convergence of the SSP(4,4) and SSP(6,4) RKDG methods

Δx	SSP(4,4)		SSP(6,4)	
	Error	Order	Error	Order
2.00	2.27E−05	···	2.22E−05	···
1.00	1.66E−06	3.77	1.82E−06	3.61
0.50	1.12E−07	3.89	1.22E−07	3.89
0.25	7.12E−09	3.98	8.33E−09	3.88

6. Conclusions

In this paper, we have examined the use of stage-exceeding-order, SSP Runge–Kutta time discretization methods in conjunction with semi discrete discontinuous Galerkin methods for hyperbolic conservation laws. It was found that the use of these time schemes with DG spatial discretizations resulted in RKDG methods with improved linear stability CFL conditions compared to the "standard" RKDG methods, which use $s = k$ SSP schemes. In the majority of cases examined, the improvements in the CFL conditions were significant enough to offset the additional amount of work introduced by the increased number of stages. For second- and third-order RKDG methods, the optimal methods, in terms of computational savings, were obtained using $s = 3$ and $s = 5$ stages, respectively, and offered computational savings of approximately 15% and 18%, respectively, over the standard $s = k$ methods. More substantial savings were realized in the fourth-order case using the $s > 4$ schemes, which gave efficiency improvements of roughly 25% over the $s = 4$ case. Numerical examples demonstrated the robustness and efficiency of these schemes and verified the stability constraints obtained from analysis. Although the test cases examined here were scalar equations in one-dimension, the schemes can just as effectively be used in the case of systems of equations and multi-dimensional problems, see for example [16].

Acknowledgments

This work was supported under the Morphos 3D Development Project funded by the US Army Corps of Engineers, Mobile District contract W91278-05-D-0018/003 through Woolpert Inc. The third author was partially supported by NSF Grant DMS-0411413.

References

[1] V. Aizinger, C. Dawson, A discontinuous Galerkin method for two-dimensional flow and transport in shallow water, Advances in Water Resources 25 (2002) 67–84.
[2] J.C. Butcher, The Numerical Analysis of Ordinary Differential Equations: Runge–Kutta and General Linear Methods, John Wiley, Chichester, 1987.
[3] G. Chavent, B. Cockburn, The local projection $P^0 - P^1$-discontinuous-Galerkin finite element method for scalar conservation laws, Mathematical Modelling and Numerical Analysis 23 (1989) 565–592.
[4] B. Cockburn, C.W. Shu, TVB Runge–Kutta local projection discontinuous Galerkin finite element method for scalar conservation laws II: general framework, Mathematics of Computation 52 (1989) 411–435.
[5] B. Cockburn, S. Hou, C.W. Shu, The Runge–Kutta projection discontinuous Galerkin finite element method for conservation laws IV: the multidimensional case, Mathematics of Computation 54 (1990) 545–581.
[6] B. Cockburn, C.W. Shu, The Runge–Kutta local projection P^1-discontinuous-Galerkin finite element method for scalar conservation laws, Mathematical Modelling and Numerical Analysis 25 (1991) 337–361.
[7] B. Cockburn, C.W. Shu, Runge–Kutta discontinuous Galerkin methods for convection dominated problems, Journal of Scientific Computing 16 (2001) 173–261.
[8] J. Goodman, R. LeVeque, On the accuracy of stable schemes for 2D scalar conservation laws, Mathematics of Computation 45 (1985) 15–21.
[9] S. Gottlieb, C.W. Shu, Total variation diminishing Runge–Kutta schemes, Mathematics of Computation 67 (1998) 73–85.
[10] S. Gottlieb, C.W. Shu, E. Tadmor, Strong stability-preserving high-order time discretization methods, SIAM Review 43 (2001) 89–112.
[11] S. Gottlieb, On high order strong stability preserving Runge–Kutta and multi step time discretizations, Journal of Scientific Computing 25 (2005) 105–128.
[12] S. Gottlieb, Ruuth, Optimal strong-stability-preserving time-stepping schemes with fast downwind spatial discretizations, Journal of Scientific Computing 27 (2006) 289–303.
[13] I. Higueras, On strong stability preserving time discretization methods, Journal of Scientific Computing 21 (2004) 193–223.
[14] J.F.B.M. Kraaijevanger, Contractivity of Runge–Kutta methods, BIT 31 (1991) 482–528.
[15] E.J. Kubatko, J.J. Westerink, C. Dawson, *hp* discontinuous Galerkin methods for advection dominated problems in shallow water flow, Computer Methods in Applied Mechanics and Engineering, in press.
[16] E.J. Kubatko, J.J. Westerink, C. Dawson, A *p*-adaptive discontinuous Galerkin method for shallow water hydrodynamics and transport, International Journal for Numerical Methods in Fluids, in preparation.
[17] S.Y. Lin, Y.S. Chin, Discontinuous Galerkin finite-element method for Euler and Navier–Stokes equations, AIAA Journal 31 (1993) 2016–2026.
[18] R.D. Nair, S.J. Thomas, R.D. Loft, A discontinuous Galerkin global shallow water model, Monthly Weather Review 133 (2005) 876–888.

[19] J.F. Remacle, J.E. Flaherty, M.S. Shephard, An adaptive discontinuous Galerkin technique with an orthogonal basis applied to compressible flow problems, SIAM Review 45 (2003) 53–72.
[20] S.J. Ruuth, Global optimization of explicit strong-stability-preserving Runge–Kutta methods, Mathematics of Computation 75 (2006) 183–207.
[21] S.J. Ruuth, R.J. Spiteri, High-order strong-stability-preserving Runge–Kutta methods with downwind-biased spatial discretizations, SIAM Journal on Numerical Analysis 42 (2004) 974–996.
[22] S.J. Ruuth, R.J. Spiteri, Two barriers on strong-stability-preserving time discretization methods, Journal of Scientific Computing 17 (2002) 211–220.
[23] D. Schwanenberg, M. Harms, Discontinuous Galerkin finite-element method for transcritical two-dimensional shallow water flows, Journal of Hydraulic Engineering 130 (2004) 412–421.
[24] C.W. Shu, S. Osher, Efficient implementation of essentially non-oscillatory shock-capturing schemes, Journal of Computational Physics 77 (1988) 439–471.
[25] R.J. Spiteri, S.J. Ruuth, A new class of optimal high-order strong-stability-preserving time discretization methods, SIAM Journal on Numerical Analysis 40 (2002) 469–491.
[26] R.J. Spiteri, S.J. Ruuth, Non-linear evolution using optimal fourth-order strong-stability-preserving Runge–Kutta methods, Mathematics and Computers in Simulation 62 (2003) 125–135.
[27] H.Z. Tang, G. Warnecke, A Runge–Kutta discontinuous Galerkin method for the Euler equations, Computer and Fluids 34 (2005) 375–398.
[28] M. Wierse, A new theoretically motivated higher order upwind scheme on unstructured grids of simplices, Advances in Computational Mathematics 7 (1997) 303–335.
[29] P. Zhang, R.X. Liu, Generalization of Runge–Kutta discontinuous Galerkin method to LWR traffic flow model with inhomogeneous road conditions, Numerical Methods for Partial Differential Equations 21 (2005) 80–88.